Separation and Purification Technology 320 (2023) 124095

Contents lists available at ScienceDirect

Separation and Purification Technology

journal homepage: www.elsevier.com/locate/seppur

Mass transfer mechanism and model of CO_2 absorption into a promising DEEA-HMDA solvent in a packed column

Hong Quan [a], Chunliang Shang [a], Liju Bai [a], Zihan Fan [a], Yufan Dong [a], Shoulong Dong [a], Stefania Moioli [d], Miyi Li [a,*], Paitoon Tontiwachwuthikul [c,*], Helei Liu [a,b,c,*]

[a] School of Chemistry and Chemical Engineering, Beijing Institute of Technology, Beijing 102488, P. R. China
[b] Key Laboratory of Low-Carbon Conversion Science & Engineering, Shanghai Advanced Research Institute, Chinese Academy of Sciences (Shanghai Advanced Research Institute, Chinese Academy of Sciences, Shanghai 201210, P. R. China
[c] The Clean Energy Technologies Research Institute (CETRI), University of Regina, 3737 Wascana Parkway, Regina, Saskatchewan, S4S 0A2, Canada
[d] GASP, Group on Advanced Separation Processes and GAS Processing, Dipartimento di Chimica, Materiali e Ingegneria Chimica "Giulio Natta", Politecnico di Milano, Piazza Leonardo da Vinci 32, I-20133 Milano, Italy

ARTICLE INFO

Keywords:
CO_2 absorption
DEEA-HMDA
Mass transfer
Packed column
Model

ABSTRACT

Mass transfer performance plays an important role in solvent evaluation as well as design and scale-up of CO_2 absorption process. The mass transfer process of CO_2 absorption into blended DEEA -HMDA solution was studied over different operating conditions in a lab-scale absorption column packed with Sulzer DX structured packing. The effect of those operating parameters on $K_G a_v$ was fully investigated and discussed in this work. Meanwhile, mass transfer mechanism of CO_2 absorption into blended DEEA-HMDA solution was comprehensively presented by identifying the rate-controlling step of mass transfer and the reaction zone of CO_2 with amines, which could provide the operation guideline for running plans. In addition, a new $K_G a_v$ model was proposed and developed on basis of the observed experimental value of $K_G a_v$, which gave a much better predication performance in comparison with empirical Kohl-Risenfield-Astarita model and Sheng model with respect to AAD.

1. Introduction

The rapid growth of carbon dioxide (CO_2) emissions has been widely recognized as a serious global issue, lots of countries have implemented the corresponding carbon reduction policies[1]. The increase of CO_2 emissions could be mainly attributed to the consumption of fossil fuels. Specifically, one of the main source of CO_2 coal-fired power plants [2–4]. Therefore, the removal of CO_2 from flue gases emitted from coal-fired power plants is one of the most appropriate technologies for carbon capture and storages (CCS) [5–7]. At present, some main technologies for CO_2 capture including absorption, adsorption and membrane technology are most commonly used [8]. The amine-based CO_2 capture has developed into a relatively mature and commercialized carbon capture technology[9].

The widely used amine solvent was simply classified into three main categories as primary amine, secondary amine, tertiary amine. Monoethanolamine (MEA) as the conventional primary amine was considered as an excellent CO_2 absorber [10–12,5], which exhibited a fast absorption rate. However, disadvantages of MEA are small CO_2 absorption capacity, high desorption energy consumption and strong corrosion [13]. The tertiary amine (methyldiethanolamine) MDEA performed a large CO_2 absorption capacity, low desorption energy consumption and high degradation resistance, but its reaction rate with CO_2 was low[14]. Blended amines through combining both advantages of different amines, have been shown to be a promising direction of development for new CO_2 absorbents[15]. Luo et al.[16] studied the CO_2 absorption capacity of PZ mixed with MEA/MDEA/2-amino2-methyl-propanol (AMP). The results showed that the blends had higher absorption rate and larger absorption capacity.

Samanta et al.[6] found that the absorption rate of blended AMP-PZ solution was significantly higher than that of single AMP solution. Shi et al.[17] investigated a novel tri-solvent MEA-EAE (2-(ethylamino) ethanol)-AMP, in which the addition of EAE increased CO_2 loading and reduced absorption heat, while the addition of AMP significantly reduced the overall heat duty and enhanced cyclic capacity.

1,6-hexamethyl diamine (HMDA) containing two primary amine groups as shown in Fig. 1 was a typical primary amine HMDA which indicated the fast reaction rate and CO_2 absorption capacity. Prachi et al.

* Corresponding authors.
E-mail addresses: miyilimiyi_li@bit.edu.cn (M. Li), paitoon@uregina.ca (P. Tontiwachwuthikul), lhl0925@hotmail.com, hl_liu@bit.edu.cn (H. Liu).

https://doi.org/10.1016/j.seppur.2023.124095
Received 1 March 2023; Received in revised form 8 May 2023; Accepted 12 May 2023
Available online 18 May 2023

[19] studied the reaction kinetics of HMDA using a stirred cell reactor. It was found that the reaction of HMDA two amine groups to CO_2 was independent of each other, and the reactivity was more than five times that of MEA.

N, *N*-Diethylethanolamine (DEEA) is a tertiary amine with a high CO_2 capacity and low regenerative energy[20], which was presented in Fig. 1. The blended solvent of DEEA and HMDA could give an excellent carbon capture performance with the desired absorption and desorption behaviors, which could be treated as one of potential applicable solvents for CO_2 capture, which had been confirmed by the work of Kumar et al. [18]. In addition, Parag et al.[20] proved that with the addition of HMDA, the CO_2 absorption rates in the blend (DEEA + HMDA) were much higher than those in DEEA. Therefore, the blended DEEA-HMDA solvent was selected as the object of this work.

Before its large-scale industrialization and commercial application, large amount of fundamental research work of promising solvents should be clarified. The studies on solvent development involve a wide range of aspects such as solvent screening, mass transfer, equilibrium solubility, reaction kinetics, solvent stability, etc. Among them, mass transfer was of particular interest and played an important role in solvent evaluation as well as design and scale-up of CO_2 absorption process [6,21,22]. To evaluate the mass transfer performance, the total volume mass transfer coefficient (K_Ga_v) was commonly utilized as an indicative parameter [23–25]. Fu et al. [26] studied mass transfer performance for both MEA and diethylenetriamine (DETA) solutions in a column packed with random packing. Wen et al. [27] investigated the mass transfer process of 1DMA2P-CO_2 system in random packing and established a prediction model with the average absolute deviation (AAD) of 9.80 %. Ling et al. [15] elaborated the mass transfer process of CO_2 absorbed by blended MEA-1DMA2P solvent and developed a prediction empirical model with an average absolute relative error (AARE) of 9.03 %. In order to understand the variation of K_Ga_v under different operating conditions, the mass transfer mechanism is often explained as a theoretical basis. However, Ling et al.[28] explained the influence of inert gas flow rate on K_Ga_v of CO_2 absorption in DMEA solution, and directly based on the references concluded that the mass transfer process was controlled by liquid film. Sheng et al.[29] used the same method to explain why mass transfer resistance mainly exits in liquid film in blende PZ-DETA and AEPZ-DETA solvent system. For different amines, it is not accurate to determine mass transfer resistance only from experience and references. Therefore, it is very necessary to find a method to accurately judge the mass transfer rate control steps of different amine solvent systems under different operating conditions.

In this work, the mass transfer performance with respect to K_Ga_v of CO_2 absorption into blended DEEA -HMDA solution was studied over different operating conditions ((i.e., liquid flow rate, gas flow rate, and CO_2 loading in lean solvent) in a lab-scale absorption column packed with Sulzer DX structured packing. In addition, mass transfer mechanism of CO_2 absorption into blended DEEA-HMDA solution in the packed column was proposed and comprehensively presented by identifying the rate-controlling step of mass transfer and the reaction zone of CO_2 with amines, which could provide a better understanding of mass transfer process and the operation guideline for running plans. Finally, a new proposed K_Ga_v model, Kohl-Risenfield-Astarita model[30–32], Sheng model[29] were developed to predict the K_Ga_v. The work of this study provides guidance and data support for solvent evaluation as well as design and scale-up of CO_2 absorption process of blended DEEA-HMDA solvent.

2. Mass transfer in packed columns

2.1. Mass transfer theory

CO_2 absorption into amine solutions could be described by using the two-film theory[23]. Mass transfer happens when CO_2 moved from the gas phase across a stagnant film into the liquid phase due to the driving force generated from a chemical potential gradient between gas and liquid phases, as shown in Fig. 2.

The mass transfer behavior of gas–liquid represented by the overall mass transfer coefficient K_G could expressed by the following Eq. [33]:

$$\frac{1}{K_G}=\frac{1}{k_G}+\frac{He_{CO_2}}{k_L} \tag{1}$$

where, k_G represents mass transfer coefficient of gas phase, and k_L is mass transfer coefficient of liquid phase, He_{CO_2} denotes Henry's constant for the diffusion of CO_2 into amine solutions.

Mass transfer process accompanied chemical reactions differed from physical absorption. Chemical reactions could accelerate CO_2 into the solution and store CO_2 in the solution by forming chemical bonds through chemical reactions [34]. In case of mass transfer with chemical absorption, such as CO_2 absorption into an amine solution, K_Ga_v could be expressed as a function of enhancement factor (E)[21] which referred to the enhancement of mass transfer contributed by chemical reactions compared with pure physical absorption.

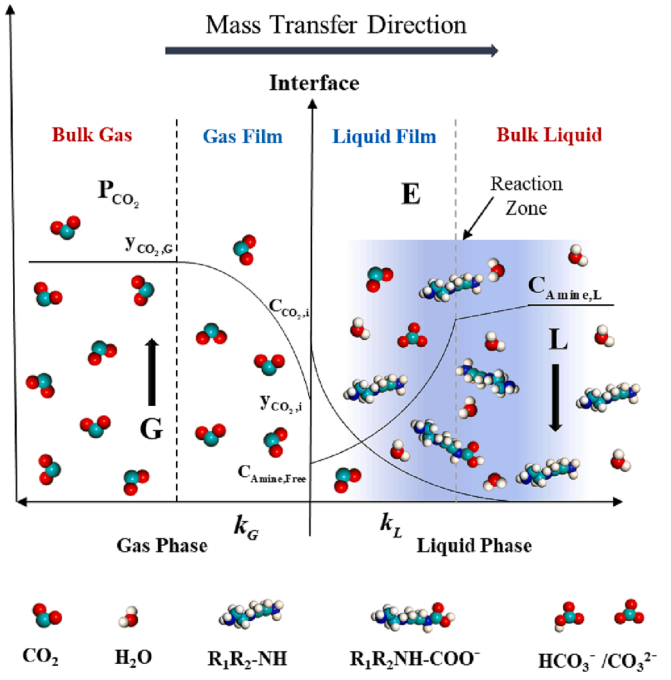

Fig. 2. CO_2 absorption into amine solutions based on two-film theory model.

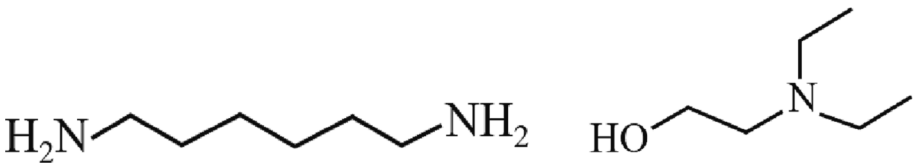

Fig. 1. The molecular structure of HMDA and DEEA[18].

$$\frac{1}{K_G a_v} = \frac{1}{k_G a_v} + \frac{He_{CO_2}}{E \cdot k_L^0 a_v} \tag{2}$$

where, k_L^0 is physical liquid-phase mass transfer coefficient without chemical reaction, a_v is the effective gas–liquid interfacial area (m^2/m^3), He_{CO_2} represents the Henry's constant.

The Henry's constant can be described by the ratio of gas- liquid partial pressure to physically dissolved gas concentration in the solution as follows [15]:

$$He_{CO_2} = \frac{P_{CO_2}}{[CO_2]} \tag{3}$$

where, P_{CO_2} is the partial pressure of CO_2 (kPa), $[CO_2]$ represents CO_2 concentration in the interface of gas–liquid.

2.2. Determination of $K_G a_v$ in a packed column

Based on the above discussion, $K_G a_v$ could describe the mass transfer behaviors, that was commonly considered to be convenient and effective to evaluate the mass transfer performance of CO_2 absorption in packed columns[23,26]. Based on the two-film theory, mass transfer occurs when CO_2 from the gas phase crosses the gas–liquid interface into the liquid phase. The driving force of mass transfer behavior was the concentration difference between gas and liquid phase, which causes component CO_2 to transfer from gas phase to liquid phase. The mass transfer flux of component CO_2 at the gas–liquid interface can be written as follows:

$$N_{CO_2} = K_G P\left(y_{CO_2} - y^*_{CO_2}\right) \tag{4}$$

where, N_{CO_2} is the mass transfer flux of CO_2, K_G *is* the overall gas-phase mass transfer coefficient, P is the total solution pressure, y_{CO_2} is the mole fraction of CO_2 in gas phase, $y^*_{CO_2}$ is the equilibrium concentration of CO_2 at the gas–liquid interface.

In packed column, the effective gas–liquid interfacial area (a_v) is considered another important factor, which is difficult to be determined [21]. Therefore, mass transfer flux of component CO_2 per unit volume can be expressed as[27]:

$$N_{CO_2} a_v = K_G a_v P\left(y_{CO_2} - y^*_{CO_2}\right) \tag{5}$$

$y^*_{CO_2}$ can be obtained by using the Henry's law, as shown in Eq. (6).

$$y^*_{CO_2} = \frac{P_{CO_2}}{He_{CO_2}} \tag{6}$$

where, P_{CO_2} is the partial pressure of CO_2.

Considering a small differential height of packing (dZ), the overall differential mass balance can be given as follows:

$$N_{CO_2} a_v dZ = G dY_{CO_2} \tag{7}$$

where, G is the molar flow rate of inert gas, Y_{CO_2} is the molar ratio of CO_2 in the gas phase.

By submitting Eq. (5) into Eq. (7), the total volume mass transfer coefficient $K_G a_v$ can be defined as:

$$K_G a_v = \frac{G}{P\left(y_{CO_2} - y^*_{CO_2}\right)} \frac{dY_{CO_2}}{dZ} \tag{8}$$

The concentration gradient (dY_{CO_2}/dZ) can be calculated by measuring the CO_2 concentration along the column height and subsequently plotting as the concentration profile as presented in Fig. 3.

The value of $K_G a_v$ was obtained by taking the geometric average of 6 different column heights as Eq. (9)

$$K_m = \sqrt[6]{K_1 K_2 K_3 K_4 K_5 K_6} \tag{9}$$

3. Experimental sections

3.1. Chemicals

Monoethanolamine (98 %), N, *N*-Diethylethanolamine (99 %) and 1,6-hexamethyldiamine (AR ≥ 98%) were purchased from Macklin Co., ltd., China. Carbon dioxide and nitrogen gas (99.999 %) were purchased from Beijing Wansheng Da Feng Gas Co., ltd, China. All materials used in

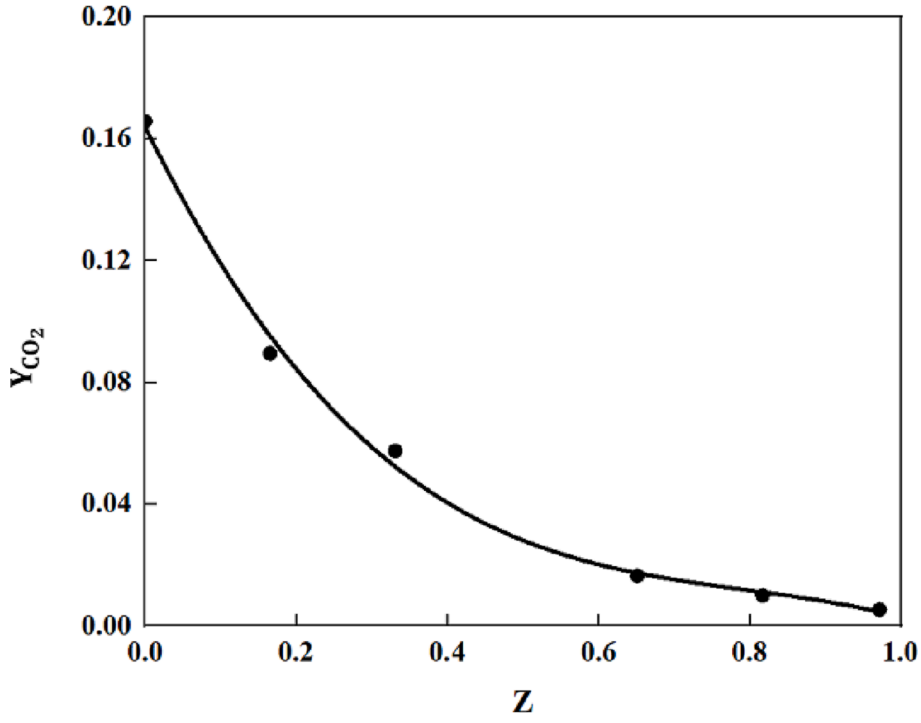

Fig. 3. Fitting curve of CO_2 concentration as a function of packed column height.

this work were received without further purification.

3.2. Mass transfer in a packed column

In order to determine the mass transfer performance of CO_2 absorbed by blended DEEA-HMDA solvent, the experimental set-up was designed as presented in Fig. 4, which was mainly composed of a packed column, gas mixture section, water bath, amine tanks. The absorption column is composed of two sections of double-layer vacuum glass columns with diameter of 0.026 m and height of 0.97 m. It is packed with the structured packing (DX-type with specific surface area of 1000 m^2/m^3), which was purchased from Tianjin Pushang Technology Co., ltd, China. The column consisted of five CO_2 concentration and temperature measurement points distributed on both sides of the column.

The experimental procedure was briefly presented as the following. Firstly, the simulated flue gas with 15 % CO_2 was obtained by employing the two gases mass flow meter to control the flow rate of N_2 and CO_2, respectively. The mixed gases were passed through the water bath and then were introduced into the packed column from the bottom. The lean amine was pumped from the amine tank through the water bath into the packed column from the top. The gases were in countercurrent contact with the lean amine solution from the top of the column to achieve the CO_2 removal. The off-gas was released to the atmosphere from the top of column after throughout the condenser. The rich amine was collected from the bottom of column and was stored into rich amine tank. Meanwhile, the temperature and CO_2 concentration were also detected at different column heights. After CO_2 absorption into the column, the solvent was sent for desorption for reuse.

3.3. CO_2 analysis in gas phase

The gases from the column were introduced through a drying tube to remove the moisture. The dried gas was sent to CO_2 analyzers (MinIR, British GSS Company) to obtain CO_2 concentration in gas phase.

3.4. CO_2 analysis in liquid phase

Amine concentrations and CO_2 loading were measured with a titration device in Fig. 5. The principle is acid-base titration, through the known concentration of hydrochloric acid and the volume consumed in the titration process to obtain the concentration of amine, and then through the right volume of the trachea to obtain CO_2 loading [37]. The

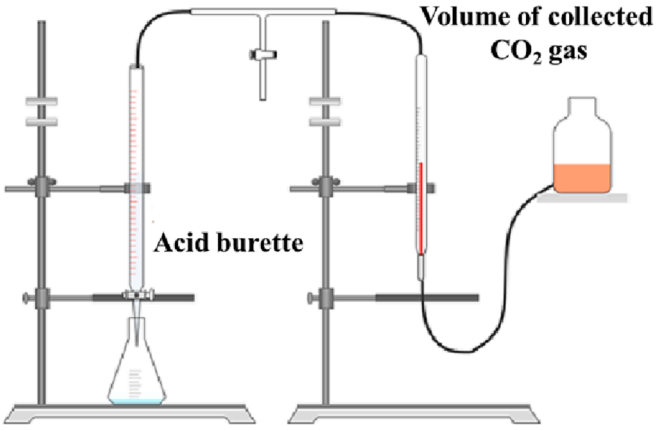

Fig. 5. Schematic diagram of CO_2 loading titration device[36].

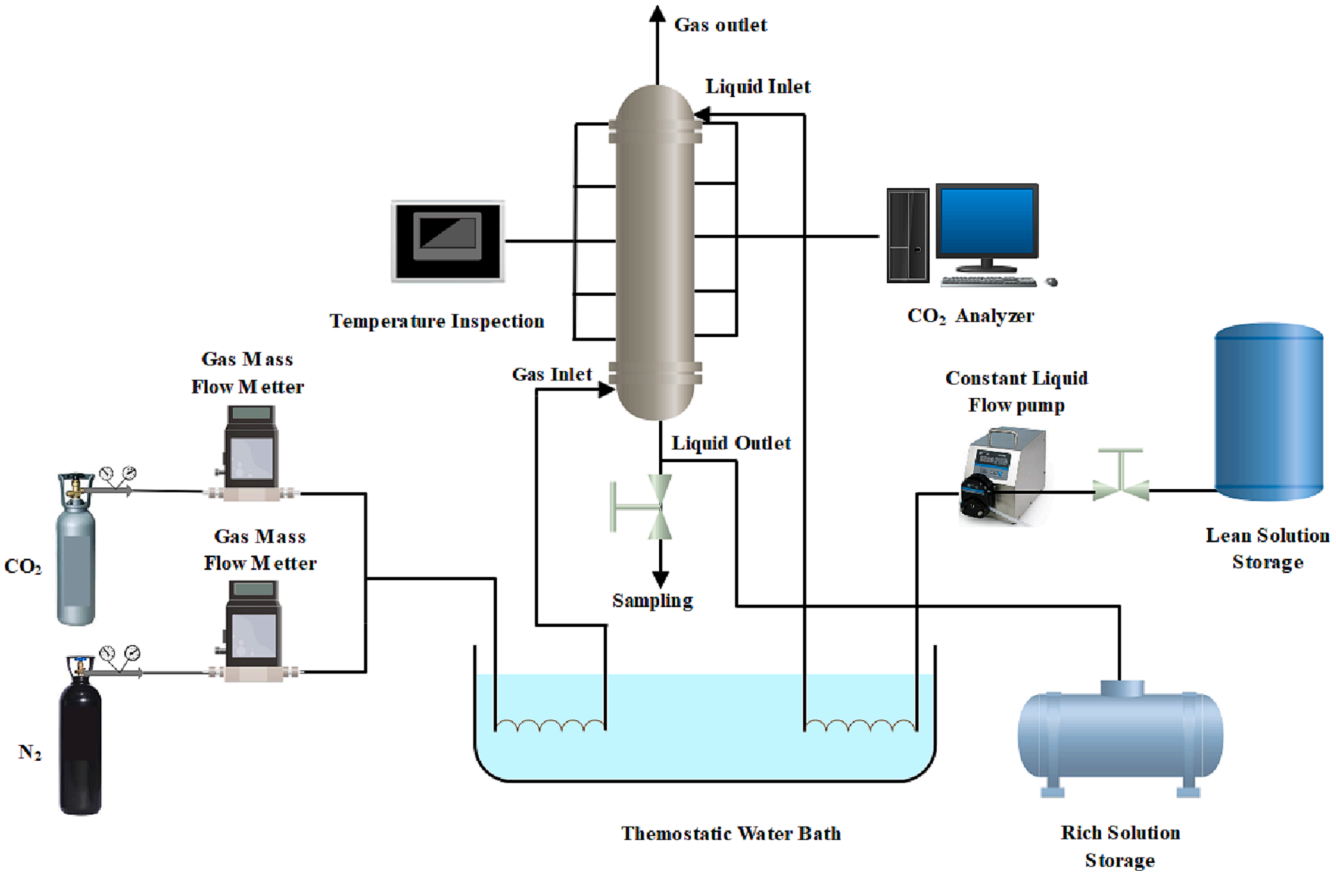

Fig. 4. Schematic diagram of mass transfer experiment device[35].

specific calculation formula is as follows:

$$\alpha = \frac{V_{CO_2} - V_{HCl}}{22.4 \times C_{amine} \times V_{amine}} \times \frac{273.15}{273.15 + T} \quad (10)$$

where α is the CO_2 loading (mol/mol), C_{amine} is the molarity of amine sample (mol/L), V_{amine} is the volume of amine solution (ml), V_{CO_2} and V_{HCl} are the reduced volume of the trachea and the acid burette, respectively.

In order to ensure the reliability of the experimental data, material balance of the whole packed column as shown in Fig. 6 was presented by giving CO_2 mass balance of both liquid and gas.

4. Results and discussion

4.1. Operation parameters effect on $K_G a_v$

In the work, the experimental data extracted from this experimental setup was reliable as shown in Fig.7, which CO_2 absorbed into liquid phase gave a great agreement with CO_2 lost from gas phase with absolute average deviation (AAD) of 3.18 %.

Mass transfer behaviors of CO_2 absorption into blended amines into a packed column was complicated since it was affected by couple of operation parameters. In order to comprehensibly assess the effect of those parameters on mass transfer coefficient, a series of mass transfer experiments were designed and conducted with different operation range of ratio of DEEA-HMDA, feed temperature (T), gas flow rate (G), liquid flow rate (L), CO_2 partial pressure (P_{CO_2}), which were shown in Table 1. The $K_G a_v$ for each run was calculated as presented in section 2.2. All experimental results were presented in Table 2.

4.1.1. Effect of concentration ratio of DEEA and HMDA

The blended solvents consisted of DEEA and HMDA, which gave different CO_2 absorption rates and mechanisms. Thus, the composition of blended solvent would play a significant role in mass transfer behavior of CO_2 in liquid phase. In order to explore the contribution of components to mass transfer performance and optimize the ratio of DEEA-HMDA in mixed amine solution, mass transfer experiment of CO_2 absorption into different ratio of DEEA-HMDA were conducted in this work. And, all results could be observed in Fig. 8.

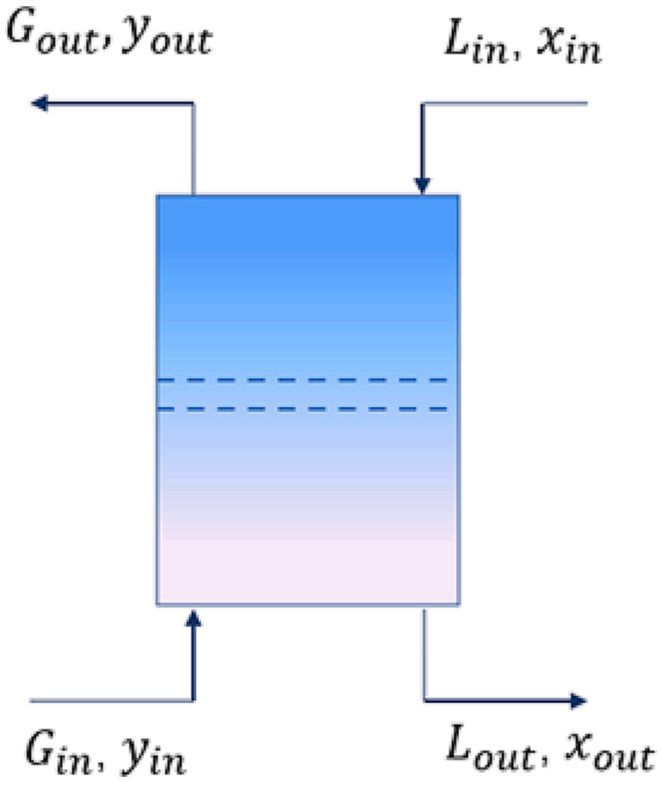

Fig. 6. The diagram for mass balance of the column.

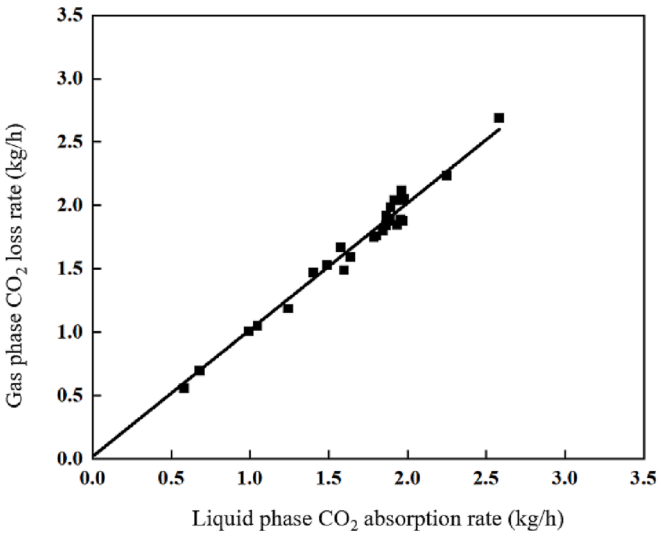

Fig. 7. Gas-liquid material balance for all absorption experiments.

Table 1
The range of operation parameters.

Parameters	Conditions
Inert gas flow rate(kmol/m^2·h)	12.63–32.83
Liquid flow rate (m^3/m^2·h)	3.96–9.5
CO_2 partial pressure (kPa)	7.5–15
CO_2 loading (mol/mol)	0.05–0.45
Feed temperature (K)	298.15–318.15
DEEA concentration (mol/L)	0.6–2.4
HMDA concentration (mol/L)	0.6–2.4

The values of $K_G a_v$ increased with the increasing concentration of primary HMDA. It is worth noting that $K_G a_v$ increases in different degree when HMDA concentration is less than or greater than 1.5 mol/L. This result could be attributable to the increased concentration of HMDA with a faster reaction rate[20] leading to higher $K_G a_v$ values. As a result, a shorter column was required to achieve a certain CO_2 removal target. However, more HMDA mean more energy consumption for desorption process, which resulted into the higher cost of regeneration. Meanwhile, the present of a tertiary amine DEEA with a higher CO_2 capacity could contribute to more CO_2 capacity, which could result in less amine consumption.

4.1.2. Effect of inert gas flow rate

Gas flow rate(G) directly affects the gas phase mass transfer coefficient (k_G) and leads to the distribution of CO_2 concentration in gas film. Thus, inert gas flow rate was regarded a vital parameter, which affected the mass transfer behavior of gas into liquid phase. In this work, the effect of inert gas flow rate on $K_G a_v$ was investigated and presented in Fig. 9. The value of $K_G a_v$ sharply increased with the increase of inert gas flow rate.

It could be explained that the increase of inert gas flow rate correspondingly increased the degree of gas-phase turbulence in the packed column, which thus strengthened the gas–liquid contact and improved mass transfer performance[38]. In addition, when the gas flow rate is small, the increase of the gas flow rate will increase the concentration distribution of CO_2 at the interface, thus leading to the increase of the gas driving force. However, as the gas flow rate increases, the friction between the rising flow gas and the falling liquid increases, and the

Table 2
The $K_G a_v$ values with different operational parameters.

NO.	DEEA concentration (mol/L)	HMDA concentration (mol/L)	Inert gas flow rate (kmol/m^2·h)	Liquid flow rate (m^3/m^2·h)	CO_2 partial pressure (kPa)	CO_2 loading (mol/mol)	Feed temperature (K)	$K_G a_v$(kmol/m^3·h·kPa)
1	2.4	0.6	22.5	6.78	15	0.1	313	0.5492
2	1.8	1.2	22.5	6.78	15	0.1	313	0.6458
3	1.2	1.8	22.5	6.78	15	0.1	313	0.8227
4	0.6	2.4	22.5	6.78	15	0.1	313	0.9143
5	1.5	1.5	12.5	6.78	15	0.1	313	0.6373
6	1.5	1.5	17.5	6.78	15	0.1	313	0.7534
7	1.5	1.5	22.5	6.78	15	0.1	313	0.7925
8	1.5	1.5	27.5	6.78	15	0.1	313	0.5753
9	1.5	1.5	32.5	6.78	15	0.1	313	0.516
10	1.5	1.5	22.5	3.96	15	0.1	313	0.6205
11	1.5	1.5	22.5	5.31	15	0.1	313	0.7504
12	1.5	1.5	22.5	6.78	15	0.1	313	0.7925
13	1.5	1.5	22.5	8.25	15	0.1	313	0.8599
14	1.5	1.5	22.5	9.5	15	0.1	313	0.9599
15	1.5	1.5	22.5	6.78	15	0.05	313	1.3473
16	1.5	1.5	22.5	6.78	15	0.15	313	0.8633
17	1.5	1.5	22.5	6.78	15	0.2	313	0.4181
18	1.5	1.5	22.5	6.78	15	0.25	313	0.3772
19	1.5	1.5	22.5	6.78	15	0.35	313	0.1767
20	1.5	1.5	22.5	6.78	15	0.42	313	0.1152
21	1.5	1.5	22.5	6.78	7.5	0.1	313	0.627
22	1.5	1.5	22.5	6.78	10	0.1	313	0.632
23	1.5	1.5	22.5	6.78	12.5	0.1	313	0.639
24	1.5	1.5	22.5	6.78	15	0.1	313	0.7925
25	1.5	1.5	22.5	6.78	15	0.1	303	0.8933
26	1.5	1.5	22.5	6.78	15	0.1	308	0.9783
27	1.5	1.5	22.5	6.78	15	0.1	313	0.7925
28	1.5	1.5	22.5	6.78	15	0.1	318	1.0464
29	1.5	1.5	22.5	6.78	15	0.1	298	0.7679

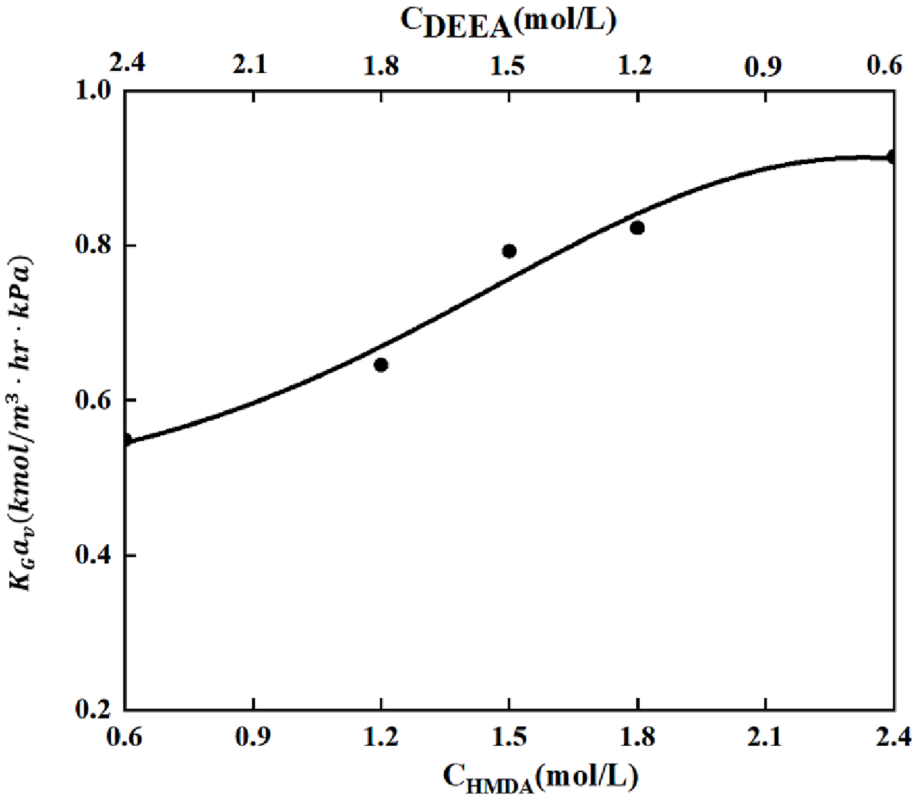

Fig. 8. Effect of different proportions of DEEA-HMDA solution on $K_G a_v$. (Inert gas flow rate = 22.5 kmol/m^2·h, Liquid flow rate = 6.78 m^3/m^2·h, Feed temperature = 313 K, CO_2 loading = mol CO_2/mol amine, CO_2 partial pressure = 15 kPa.

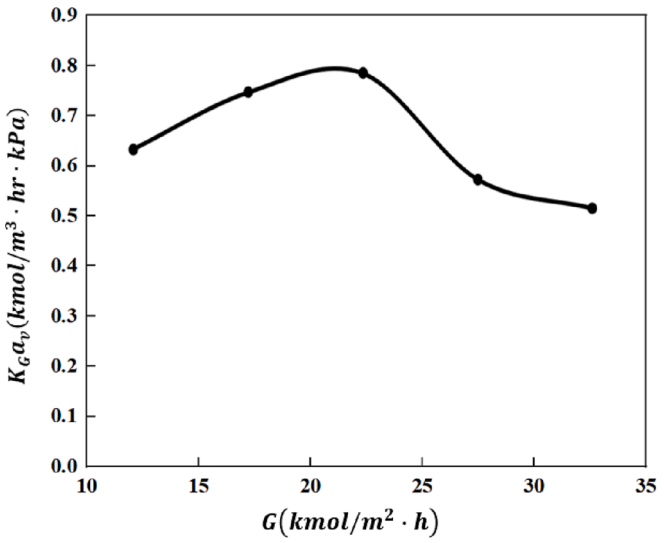

Fig. 9. Effect of inert gas flow rate on $K_G a_v$. Liquid flow rate = 6.78 m^3/m^2·h, Concentration of DEEA-HMDA = 3 mol/L (1:1), CO_2 loading = 0.1 mol CO_2/mol amine, CO_2 partial pressure = 15 kPa, Feed temperature = 313 K.

liquid flow becomes obstructed. The high gas flow rate in the packed column may start to entrain the liquid solvent, leading to the decline of the mass transfer efficiency of the whole column. Once the inert gas flow is too large, the residence time of gas liquid in the packed column will be shortened sharply. The results showed that the mass transfer performance of CO_2 in amine solvent decreased [12]. This phenomenon was observed and confirmed by experimental results as presented in Fig. 9.

4.1.3. *Effect of liquid flow rate*

The liquid flow rate (L) directly impacts on the physical liquid-phase mass transfer coefficient k_L^0 and amount of free amine available for reaction with CO_2. It was believed that L would play a vital effect on the mass transfer behavior of CO_2 absorption into amine. In this work, effect of liquid flow rate on $K_G a_v$ was also fully investigated. It can be seen from Fig. 10 that $K_G a_v$ monotonically increased with the increase of liquid flow rate.

With the increase of liquid flow rate, liquid in the column was updated faster. The number of fresh amine molecule in liquid film was relatively increased, which thus enhanced CO_2 absorption into liquid phase[15]. Meanwhile, the higher liquid flow rate could increase the degree of liquid turbulence in the packed column which could also strengthen gas–liquid contact to enhance mass transfer performance. However, with the increase of liquid flow rate, CO_2 is almost completely absorbed into the solution, the absorption process reaches equilibrium, and $K_G a_v$ would reach a stable value or decrease trend. Therefore, it is very important to select a suitable liquid flow rate[9,11].

In addition, although the higher liquid flow rate can significantly improve the removal rate of CO_2 in the packed column, CO_2 loading of the solution would be reduced due to the shorter residence time of liquid–gas. Obviously, free amine was not fully utilized, which thus would lead to the more consumption of solvent and pump transmission power cost. Therefore, the optimal liquid flow rate should be selected by taking all potential factors into consideration.

4.1.4. *Effect of CO_2 partial pressure*

Another operational parameter CO_2 partial pressure determines the driving force of gas phase and has a direct influence on the gas phase mass transfer coefficient k_G. In this work, effect of CO_2 partial pressure on $K_G a_v$ was fully investigated and comprehensively presented as shown in Fig. 11. As seen from Fig. 11, the increasing trend as function of CO_2 partial pressure was observed as expected. This could be explained that the increase of CO_2 partial pressure resulting in the increase of inlet CO_2 concentration would increase the high driving force gas phase, which eventually contributed to the higher mass transfer coefficient. When the CO_2 partial pressure was lower than 12.5 kPa, the value of $K_G a_v$ increased slightly.

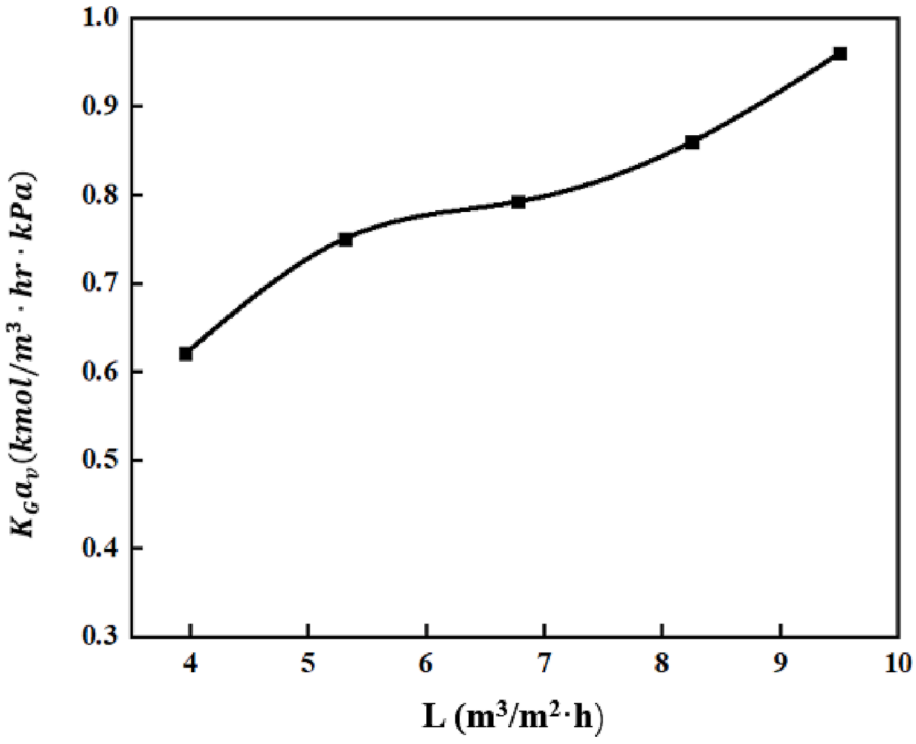

Fig. 10. Effect of liquid feed flow rate on $K_G a_v$. Inert gas flow rate = 22.5 kmol/m^2·h, Concentration of DEEA-HMDA = 3 mol/L (1:1), CO_2 loading = 0.1 mol CO_2/mol amine, CO_2 partial pressure = 15 kPa, Feed temperature = 313 K.

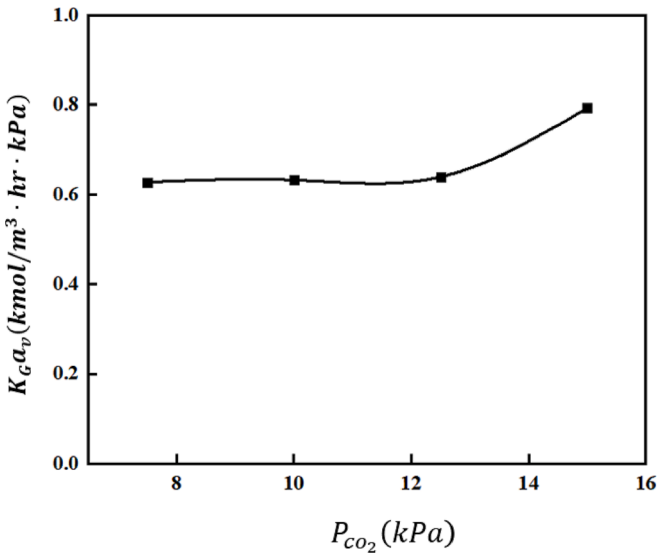

Fig. 11. Effect of CO_2 partial pressure on $K_G a_v$. Inert gas flow rate = 22.5 kmol/m^2·h, Liquid flow rate = 6.78 m^3/m^2·h, Concentration DEEA-HMDA = 3 mol/L (1:1), CO_2 loading = 0.1 mol CO_2/mol amine, Feed temperature = 313 K.

4.1.5. *Effect of feed temperature*

Temperature affects the diffusion rate of CO_2 molecules in the gas film and the reaction kinetics of CO_2 absorption into amine solutions, which was taken as a key parameter. This section mainly explored the impact of temperature on $K_G a_v$. Detailed results of investigations were fully presented in Fig. 12.

It could be seen from Fig. 12 that $K_G a_v$ exhibited an increase trend as a function of temperature. Firstly, the increase of temperature would enhance molecular movement, which leaded to a positive effect on the diffusivity. Secondly, the process of CO_2 absorption involved the chemical reaction of amine with CO_2, which was significantly affected by temperature. The high temperature contributed to the fast reaction rate, which would enhance mass transfer performance. As a result of both promotions of diffusivity and chemical reaction, $K_G a_v$ gave the increasing trend as observed from experimental results.

Even though high temperature could give a much better performance of mass transfer, it also would have some negative effect on CO_2 capture process. One was that more solvent would be consumed since the CO_2 capability of solvent is negatively related to temperature. In addition, increase of operational temperature caused more solvent loss due to volatilization. Thus, the selection of optimal temperature should be seriously treated.

4.1.6. *Effect of CO_2 loading*

CO_2 loading determines the amount of free amine in amine solutions and has a negative influence on mass transfer performance. The lower loading of lean solution, the higher amount of the active amine and the stronger ability of CO_2 absorption. In order to comprehensively study effect of CO_2 loading on $K_G a_v$, a wide range of CO_2 loading from 0.05 to 0.49 mol CO_2/mol amine was conducted in this work. All results were displayed in Fig. 13.

The values of $K_G a_v$ exhibited a gradual decreasing trend with the increase of CO_2 loading. The reason for this phenomenon was that less free amine caused by the high CO_2 loading weakened the enhancement of reaction of CO_2 with amine. Therefore, in the operation process of treating flue gases, it was necessary to reduce the CO_2 loading of lean liquid as much as possible to enhance mass transfer efficiency. However, the desorption of rich liquid required a large vast energy. The lower loading of lean liquid from desorption, the more energy was required, which would increase operating cost. Therefore, it was essential to consider the appropriate CO_2 loading of lean liquid when designing operation process.

4.2. *Mass transfer mechanism*

For mass transfer with chemical reaction, based on the two-film theory, the process of CO_2 absorption into amine solvents can briefly

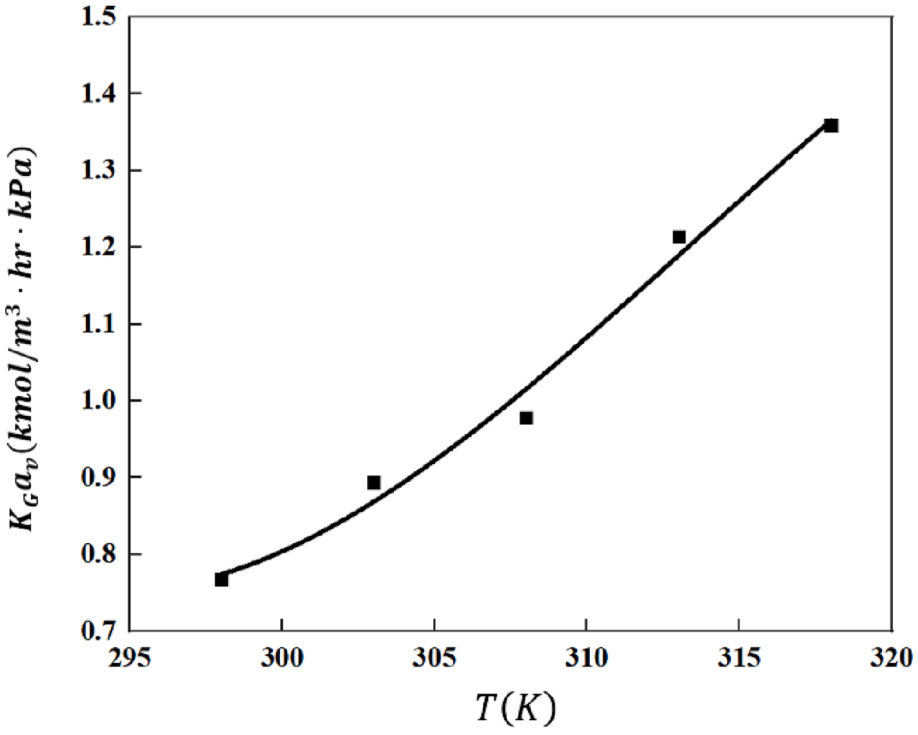

Fig. 12. Effect of feed temperature on $K_G a_v$. Inert gas flow rate = 22.5 kmol/m^2·h, Liquid flow rate = 6.78 m^3/m^2·h, Concentration of DEEA-HMDA = 3 mol/L (1:1), DEEA- HMDA = 3 mol/L (1:1), CO_2 loading = 0.1 mol CO_2/mol amine, CO_2 partial pressure = 15 kPa.

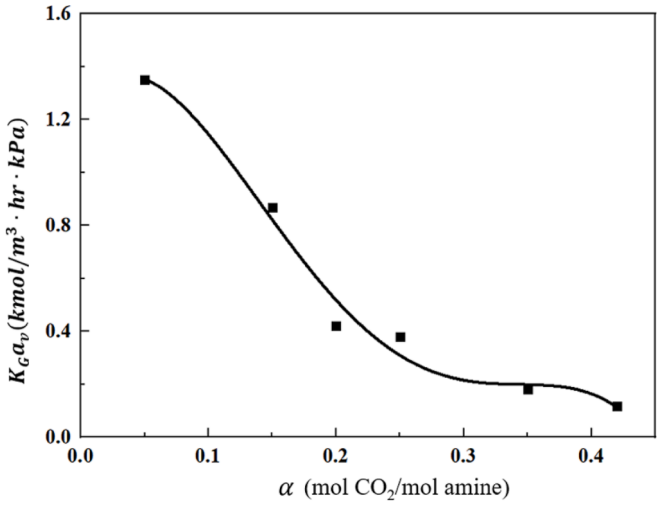

Fig. 13. Effect of CO_2 loading on $K_G a_v$. Inert gas flow rate = 22.5 kmol/m^2·h, Liquid flow rate = 6.78 m^3/m^2·h, Concentration of DEEA-HMDA = 3 mol/L (1:1), CO_2 partial pressure = 15 kPa, Feed temperature = 313 K.

be divided into three steps. Firstly, CO_2 molecules diffused from gas bulk across gas film to reach gas–liquid interface. Then, CO_2 enters the liquid from the gas–liquid interface through physical diffusion. Eventually, CO_2 was absorbed by chemical reaction with amine in liquid bulk[39].

Thus, the process of CO_2 absorption in the column was complicatedly determined by the above three steps of gas film diffusion, liquid film diffusion, and chemical reaction, which dramatically varied from the properties of solvent and operational conditions. For example, the rate controlling step of mass transfer may vary from gas film diffusion step to liquid film diffusion step as amine solvent and operational condition was different. In addition, the reaction zone may happen in liquid film or liquid bulk, which was determined by reaction rate of amine with CO_2.

Thus, it is essential to study mass transfer mechanism in order to fully identify mass transfer behavior, which could provide the operational guideline to efficiently run the plan. In order to comprehensively understand the mass transfer behaviors of CO_2 absorption into DEEA-HMDA solution in the packed column, the mass transfer mechanism was developed by fully identifying rate-control step and zone of reaction.

For CO_2 absorption into DEEA-HMDA solution, the total mass transfer coefficient could be expressed as the following Eq. [21]:

$$\frac{1}{K_G} = \frac{1}{k_G} + \frac{He_{CO_2}}{Ek_L^0} = \frac{1}{k_G} + \frac{1}{k_g^{'}} \tag{11}$$

where,He_{CO_2} is Henry's constant($kPa \bullet m^3/kmol$), k_G and $k_g^{'}$ represent gas phase and liquid phase mass transfer coefficient ($kmol/(m^2 \bullet s \bullet kPa)$), respectively, is physical liquid phase mass transfer coefficient (m/s), E is enhancement factor.

In order to identify the mass transfer of contribution of gas and liquid films, values of k_G, $k_g^{'}$, and k_L^0 can be calculated based on the mass transfer correlations proposed by researchers[40–42] as follows:

$$k_G = 5.23\left(\frac{D_G A_T}{RT}\right)\left(\frac{G}{A_T \mu_G}\right)^{0.7}\left(\frac{\mu_G}{\rho_G D_G}\right)^{0.33}(A_T d_p)^{-2} \tag{12}$$

$$k_g^{'} = \frac{\sqrt{k_2 C_{sol}^{bulk} D_{CO_2}^L}}{H_{eCO_2}} \tag{13}$$

$$k_L^0 = \left(2.4 D_{CO_2}^L\right)^{0.5} \tag{14}$$

where, D_G denotes diffusivity of the gas in the membrane pores(m^2/s), A_T represents the total packing interfacial area (m^2/m^3), G is superficial mass velocity of the gas (kg/m^2hr), μ_G denotes the viscosity of gas phase $(kg/(m{\cdot}h))$, ρ_G is density of gas phase (kg/m^3), d_p is nominal size of packing (m), R is gas constant $(kPa \bullet m^3/kmol \bullet K)$, T represents the temperature (K), $D_{CO_2}^L$ is diffusivity of CO_2 the liquid phase (m^2/s), k_2 is kinetic rate constant (m^2/s).

MEA was selected and used to validate the proposed method to determine the mass transfer mechanism. The properties data of 5 mol/L MEA was collected from references, values of $D_{CO_2}^L$ in the packed column was 1.92×10^{-9} (m^2/s) collected from the reference[43]. μ_G and ρ_G were calculated from a fitting to the viscosity and density of their pure gas. Operational parameters were used extracted from this present work. A_T and d_p were 1000 (m^2/m^3) and 0.026 m from the device used in this work. Inert gas flow rate was $29177.9 kg/m^2hr$ and temperature was 313.15 K from the experimental operating conditions. The value of k_G, $k_g^{'}$, k_L^0 and K_G were calculated and compared with results from the reference as shown in Table 3.

It can be seen from Table 3 that the calculated value of $k_g^{'}$ and K_G had an agreement with the collected values from references, respectively. Thus, it could be concluded that results extracted from proposed equations were reliable. It also could be observed from Table 3 that the mass transfer resistance of liquid accounted for 63.06 % of the total mass transfer resistance, which indicated that mass transfer rate of CO_2 into MEA solution was determined by liquid film as presented in Fig. 14. As a result, mass transfer in liquid film form MEA was a rate-controlling step. Thus, the operational parameters related to liquid phase should be seriously treated in order to enhance mass transfer behaviors of MEA in the column, which had been confirmed by many researchers.

As well known, Hatta number (Ha) was employed to identify the reaction regime in the process of mass transfer with chemical reaction. In this present work, Ha for MEA was obtained by using the following Eq. [48]:

$$Ha = \frac{\sqrt{k_2 C_{MEA} D_{CO_2}}}{k_L^0} \tag{15}$$

The Henry's constant of CO_2 in MEA solutions was obtained as $5613 kPa \bullet m^3/kmol$ from the work of Mandal et al.[49]. The values of k_2 was $13600 m^3/kmol \bullet s$ [50].

It was founded that Ha of MEA was 168.28≫2, which was considered as the fast reaction. Thus, it could be identified that the reaction zone for MEA occurred in the liquid film due to the fast reaction rate.

When the value of Ha was large enough ($3 < Ha < E_i/2$ with E_i being the value of E for the instantaneous reaction), enhancement factor E is considered equal to Ha[51]. The enhancement factor (E) could be observed as 168. 28. It could be seen from Table 3 that the value of E for MEA was acceptable in comparison with the collected value.

Liquid mass transfer resistance accounted for 63.06 % of the total mass transfer resistance. It indicated that the rate of absorption of CO_2 by lean liquid was controlled by liquid film. The enhancement factor of this process is 168.28, which proves that reaction zone CO_2 with MEA occurs in the liquid film as sated in Fig. 14. The mass transfer mechanism of MEA absorption CO_2 was clearly illustrated with a rate-controlling step of liquid film and reaction zone in liquid film.

As more CO_2 absorbed into MEA solution, ability of reaction obviously reduced, which lead to the decrease of E as shown in Table 3. The reaction regime of MEA with high CO_2 loading may vary as expected in Fig. 15 due to the decrease of E, which was different with Fig. 14. However, this phenomenon needs to be approved with further experimental investigations.

Based on the above observation, mass transfer mechanism of MEA absorption CO_2 was clearly presented based the proposed method in this work, which had been approved and confirmed with the data and observation from the references. In order to better understand the mass

Table 3
Mass transfer coefficient and kinetic parameters of MEA solution at 313 K.

C_{MEA} mol/L	$k_G \times 10^6 kmol/(m^2 \bullet s \bullet kPa)$	$k_L^0 \times 10^5 m/s$	$k_g^{'} \times 10^6 kmol/(m^2 \bullet s \bullet kPa)$	$K_G \times 10^6 kmol/(m^2 \bullet s \bullet kPa)$	E	Reference
5	3.48	6.79	2.04	1.28	168.28	This study
4.9	–		–	1.12		Han et al.[44]
5	–		2.88	–		Dugas et al.[45]
4.9	–		2.58	–		Darde et al.[46]
5	–		–	–	100.87	Dang et al.[47]

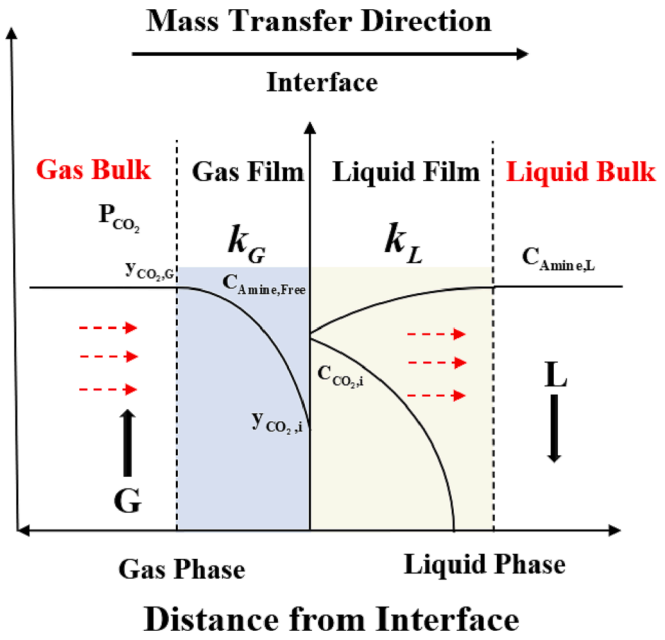

Fig. 14. The mass transfer process of CO_2 absorbed in MEA solution.

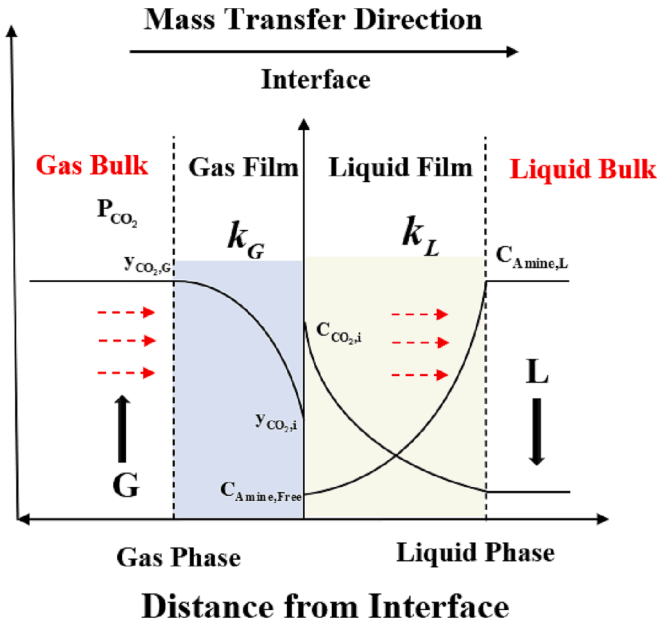

Fig. 15. The mass transfer process of CO_2 absorbed in MEA solution with high CO_2 loading.

transfer behavior of CO_2 absorption into DEEA-HMDA solution, the mass transfer mechanism for DEEA-HMDA was developed and proposed by using the same method as MEA. For DEEA-HMDA-CO_2-H_2O system, values of $D_{CO_2}^L$ and H_{CO_2} collected or calculated as $1.66 \times 10^{-9} m^2/s$ and 4385.96 kPa $\bullet$ $m^3/kmol$ from the reference[20]. k_{DEEA} and k_{HMDA} were 173 $m^3/(kmol \bullet s)$ and $4.2 \times 10^4 m^3/(kmol \bullet s)$, respectively [19,20]. All calculated results were obtained by using Eq. (13)–(16) presented in Table 4.

As shown in Table 4, liquid phase mass transfer resistance only accounted for 44.73 % of the total mass transfer resistance in the process of CO_2 absorption into DEEA-HMDA solution. It indicated that mass transfer in gas film was the rate-controlling step, which was confirmed by the experimental observation from this work. The gas flow rate played a more significant role in mass transfer coefficient in comparison with the liquid flow rate, which were consistent with the observation from Table 4. In addition, Ha number for DEEA-HMDA was also obtained as 296.5 by using Eq. (17), which was much higher than that of MEA, which was confirmed by experimental results of $K_G a_v$ in this work. This large number of Ha for DEEA-HMEA could clearly indicted the reaction zone occurred in the liquid film due to fast reaction of DEEA-HMDA with CO_2. The mass transfer mechanism of DEEA-HMDA absorption CO_2 was clearly illustrated with a rate-controlling step of gas film and reaction zone in liquid film.

Mass transfer mechanism for CO_2 absorption into blended DEEA-HMDA solution was fully developed and clearly presented in Fig. 16. It was seen that gas film residence played a key effect on the mass transfer behaviors. As a result, operational parameters closely related to gas phase would be more importantly treated when the enhancement of mass transfer was required. And, the reaction of CO_2 with amine happened immediately once CO_2 diffused into the liquid film.

As the increase of CO_2 loading, the amine was consumed. As a result, the ability of reaction was weakened due to the decrease of amine amount, which obviously had a greater impact on the entire mass transfer process and mechanism. The E of DEEA-HMDA was certainly reduced as the same trend of MEA, which leaded to the variation of reaction zone. The expected phenomena were descripted as Fig. 17, which needed to be proved by further experiments.

4.3. Mass transfer model

Accurate mass transfer coefficients are significant and helpful for column design and process optimization. Thus, the development of mass transfer model to correlate and predict $K_G a_v$ values was significantly essential. In this work, conventional and proposed models were developed in order to correlate the observed experimental results. The prediction performance of those models was discussed with respect to the absolute average deviation.

4.3.1. *Sheng model*[29]

A simplified empirical correlation with consideration of operational parameters (L, G, P_{CO2}, T) as shown in Eq. (18) was used to correlate to the obtained results of $K_G a_v$ for DEEA-HMDA.[26,38,52]

$$K_G a_v = m_1 L^{m_2} G^{m_3} e^{m_4 (W_A/W_B) W_{total}} e^{m_5 P_{CO_2} + m_6/T} \quad (16)$$

where, WA, WB, and Wtotal represent the mass fraction of activator (DEEA and HMDA), and total amine in the solution, respectively.

All coefficients were obtained by fitting all results to Eq. (16). as presented in Table 5. The values of $K_G a_v$ were predicted by using the

Table 4
Mass transfer coefficient of DEEA-HMDA solution at 313 K.

C_{DEEA} mol/L	C_{HMDA} mol/L	$k_G \times 10^6 kmol/(m^2 \bullet s \bullet kPa)$	$k_L^0 \times 10^5 m/s$	$k_g^{'} \times 10^6 kmol/(m^2 \bullet s \bullet kPa)$	$K_G \times 10^6 kmol/(m^2 \bullet s \bullet kPa)$	E
1.5	1.5	3.46	6.31	4.27	1.91	296.5

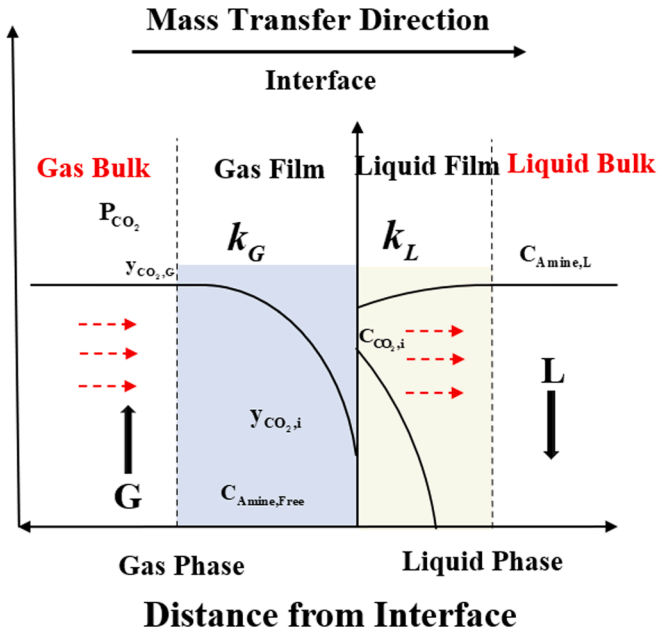

Fig. 16. The mass transfer process of CO_2 into DEEA-HMDA solution.

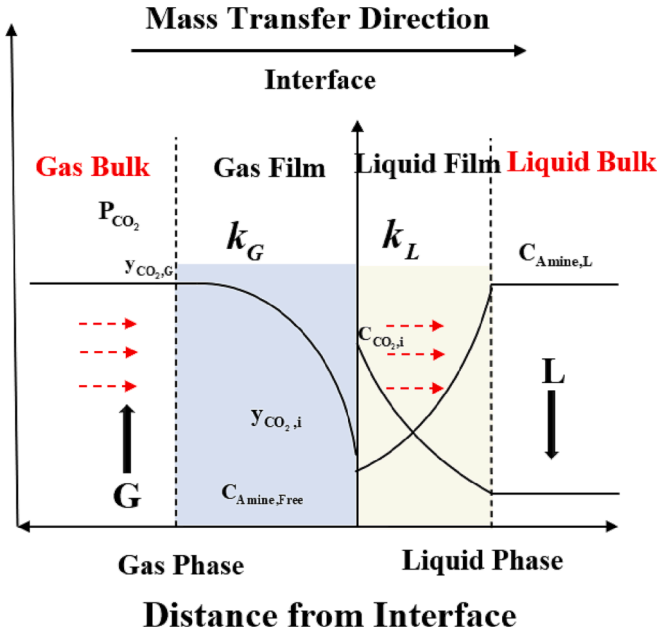

Fig. 17. The mass transfer process of CO_2 into DEEA-HMDA solution with high CO_2 loading.

Table 5
Coefficients of Sheng model.

Parameters	m_1	m_2	m_3	m_4	m_5	m_6
Value	4.946	0.4646	−0.148	−0.3464	−0.0456	228.976

obtained coefficients. All predicted results were presented and compared with experimental values as shown in Fig. 18. The calculated values of $K_G a_v$ had an agreement with the experimental values with an acceptable AAD of 8.1 %. It may be attributed to the less consideration of parameters. It could be simply summarized more parameters taken into consideration would benefit to the better prediction performance.

4.3.2. Kohl-Risenfield-Astarita model

According to the previous work[30,31], the operational parameters including liquid flow rate (L), CO_2 loading (α), CO_2 partial pressure (P_{CO_2}), amine concentration (C_{amine}) were considered as the following:

$$K_G a_v = aL^b \left[c \left(\frac{(\alpha_{eq} - \alpha) C_{amine}}{P_{CO_2}} \right) + d \right] \quad (17)$$

where, α_{eq} represents the equilibrium solubility.

The coefficients of a-d were obtained by fitting all experimental results to Eq. (18), which were listed as in Table 6.

$$K_G a_V = 0.1716 L^{0.4802} [224.8101 \frac{(\alpha_{eq} - \alpha) C}{P_{CO2}} - 0.8192] \quad (18)$$

$K_G a_v$ was predicted by using the Eq. (20), which was presented in Fig. 19. The calculated $K_G a_v$ values had a good agreement with the experimental results with an AAD of 1.57 %. In comparison with Sheng model, this model with extra parameter of CO_2 loading exhibited a much better performance in term of AAD. It could be summarized that those models with introduction of all parameters could correlate and predict the $K_G a_v$ very well, which could be treated as the direction of model development.

4.3.3. Proposed model

The two models discussed could face the need of estimation of $K_G a_v$ with AADs of 8.1 % and 1.57 %, respectively. However, only operational parameters were considered in the development of mass transfer model without taking the reaction into account, which may be the main reason for the present prediction performance without further improvement. Chemical reaction which had a significant effect on mass transfer should be considered when the correlated model was developed.

In order to better correlate experimental values of $K_G a_v$, effect of chemical reaction was introduced into the previous empirical model by employing a new parameter of mass transfer enhancement factor (E_m). The parameter of E_m was defined as the ratio of the $K_G a_v$ of amine and $K_G a_v$ of water, which could be experimentally obtained in this work. Based on the proposed idea, a new model was developed by introducing the parameter of E_m as the following:

$$K_G a_V = m_1 L^{m_2} G^{m_3} e^{m_4 (W_A/W_B) W_{total} + m_5 P_{CO_2} + m_6/T + m_7 E} \quad (19)$$

The coefficients were obtained by correlating the all observed results to Eq. (21), which were presented in Table 7.

And, values of $K_G a_v$ were represented by using Eq. (19), which were plotted and compared with experimental values as shown in Fig. 20. It could be seen that the predicted results had an excellent agreement with experimental values with an AAD of 0.11 %. The proposed model with consideration of reaction gave a better prediction performance than those of two previous models in term of AAD, which indicated that the proposed model could provide an accurate prediction of mass transfer coefficients..

For specific amine systems, the comparison results of different models are shown in Table 8.

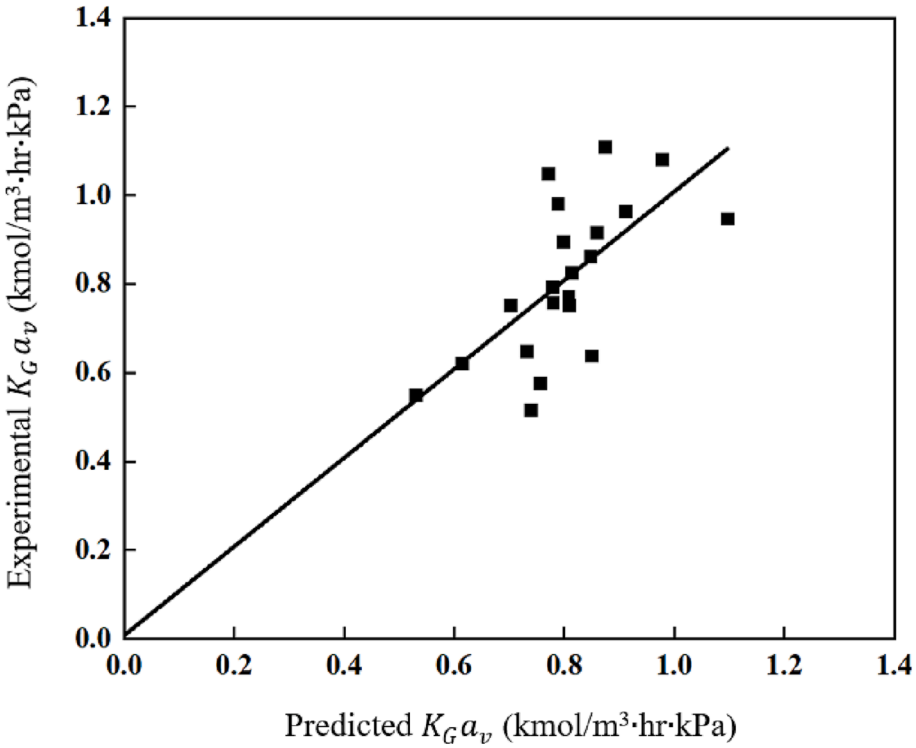

Fig. 18. Parity chart of experimental values and calculated values from Sheng model.

Table 6
Coefficients of Kohl-Risenfield-Astarita model.

Parameters	a	b	c	d
Value	0.1716	0.4802	224.8101	−0.8192

However, due to the lack of data source on physical and chemical properties, it is essential to further study the more accurate correlation of DEEA-HMDA. In addition, more research should be done to make sure the established model in this work is applicable to other cases in packed columns.

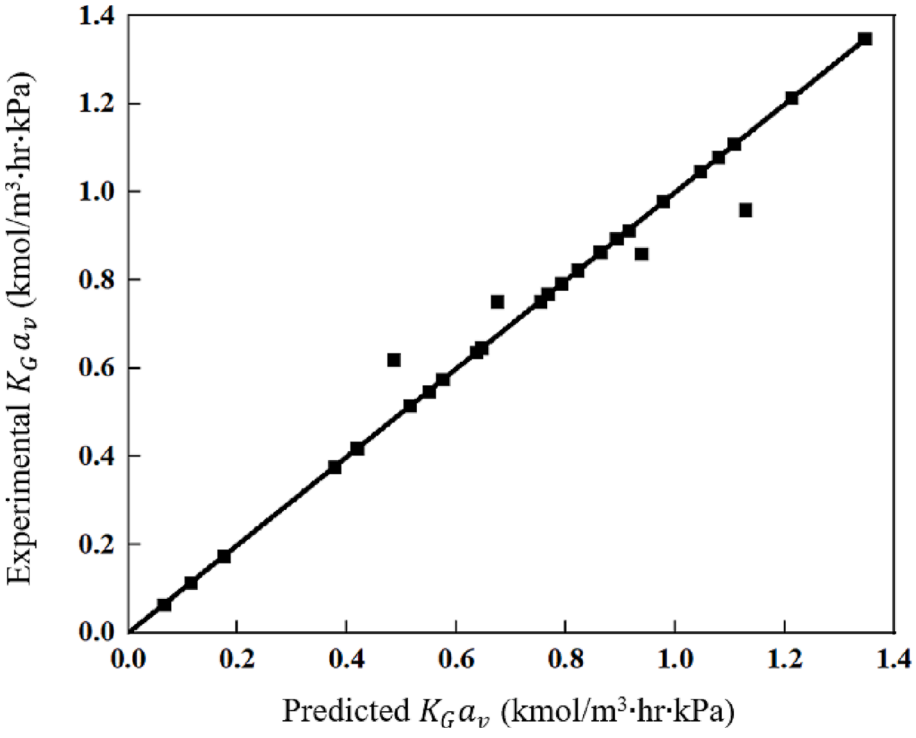

Fig. 19. Parity chart of experimental and the calculated $K_G a_v$ values.

Table 7
Coefficients of the proposed model.

Parameters	m_1	m_2	m_3	m_4	m_5	m_6	m_7
Value	0.2236	0.0068	−0.0527	−0.0363	0.0028	125.4637	0.0413

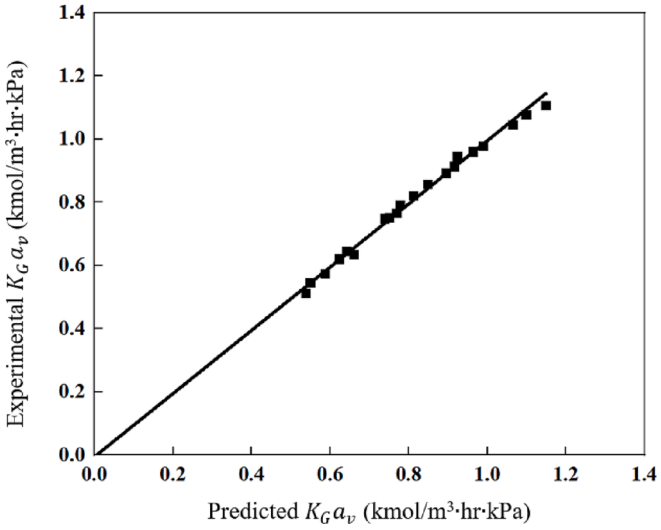

Fig. 20. Parity chart of experimental values and calculated from proposed model.

Table 8
Performance evaluation of different models for specific amine solution systems.

Amines	AAD (%)	Reference
DEEA-HMDA	0.11	This work
DETA	16	Fu et al.[26]
DMEA	4.59	Ling et al.[28]
1DME2P	9.8	Wen et al.[27]
MEA-1DMA2P	9.03	Ling et al.[15]
MEA-DMEA	8.98	Ling et al.[12]
PZ-DETA	5.35	Sheng et al.[29]

5. Conclusion

The total volume mass transfer coefficient ($K_G a_v$) of CO_2 absorption into blended 3 mol/L DEEA -HMDA solution was fully studied over different operating conditions in a lab-scale absorption column packed with Sulzer DX structured packing. The optimal ratio of 1.5 mol/LDEEA-1.5 mol/L HMDA was selected and further investigated. It was observed that the value of $K_G a_v$ increased as the increase of liquid flow rate, CO_2 partial pressure and feed temperature, decreased as CO_2 the increase of loading increased. In addition, the mass transfer of gas film was approved as the rate-controlling step in mass transfer of CO_2 into blended DEEA-HDMA solution, which was confirmed by the experimental observation. Meanwhile, the reaction zone was also identified in liquid film. The mass transfer mechanism of CO_2 absorption into DEEA-HMDA solution was proposed, which could give a better understanding of mass transfer process of CO_2 into amine solution. The proposed correlations for $K_G a_v$ with introduction of a mass transfer factor was found to give an excellent prediction performance with an AAD of 0.11 %, which exhibited a much better than 1.57 % of Kohl-Risenfield-Astarita model and 8.1 % of Sheng model, respectively.

CRediT authorship contribution statement

Hong Quan: Conceptualization, Methodology, Data curation, Writing – original draft. **Chunliang Shang:** Conceptualization, Methodology, Data curation, Writing – original draft, Investigation, Writing – review & editing. **Liju Bai:** Investigation, Writing – review & editing. **Zihan Fan:** Investigation, Writing – review & editing. **Yufan Dong:** Investigation, Writing – review & editing. **Shoulong Dong:** Supervision, Writing – review & editing. **Stefania Moioli:** Supervision. **Miyi Li:** Conceptualization, Methodology, Writing – original draft, Supervision, Writing – review & editing. **Paitoon Tontiwachwuthikul:** Conceptualization, Methodology, Data curation, Writing – original draft, Supervision, Writing – review & editing. **Helei Liu:** Conceptualization, Methodology, Data curation, Writing – original draft, Supervision, Writing – review & editing.

Declaration of Competing Interest

The authors declare that they have no known competing financial interests or personal relationships that could have appeared to influence the work reported in this paper.

Data availability

The authors do not have permission to share data.

Acknowledgement

The financial support from the National Natural Science Foundation of China (NSFC-No.22208017), the talent project from Beijing Institute of Technology (2022CX01004), the Foundation of Key Laboratory of Low-Carbon Conversion Science & Engineering, Shanghai Advanced Research Institute, Chinese Academy of Sciences (Grant No. KLLCCSE-202205) are gratefully acknowledged.

References

[1] M.U. Ali, Z. Gong, M.U. Ali, X. Wu, C. Yao, Fossil energy consumption, economic development, inward FDI impact on CO_2 emissions in Pakistan: testing EKC hypothesis through ARDL model, Int. J. Financ. Econ. 26 (2021) 3210–3221.
[2] Z. Zhang, T.N. Borhani, A.G. Olabi, Status and perspective of CO_2 absorption process, Energy 205 (2020), 118057.
[3] H. Wang, Q. Lei, P. Li, C. Liu, Y. Xue, X. Zhang, C. Li, Z. Yang, Key CO_2 capture technology of pure oxygen exhaust gas combustion for syngas-fueled high-temperature fuel cells, International Journal of, Coal Science & Technology 8 (2021) 383–393.
[4] H. Liu, V.K. Chan, P. Tantikhajorngosol, T. Li, S. Dong, C. Chan, P. Tontiwachwuthikul, Novel machine learning model correlating CO_2 equilibrium solubility in three tertiary amines, Industrial & Engineering Chemistry Research 61 (2022) 14020–14032.
[5] H. Shi, M. Cui, J. Fu, W. Dai, M. Huang, J. Han, L. Quan, P. Tontiwachwuthikul, Z. Liang, Application of "coordinative effect" into tri-solvent MEA+ BEA+ AMP blends at concentrations of 0.1+ 2+ 2~ 0.5+ 2+ 2 mol/L with absorption, desorption and mass transfer analyses, Int. J. Greenhouse Gas Control 107 (2021), 103267.
[6] S. Nakrak, T. Yurata, B. Chalermsinsuwan, P. Tontiwachwuthikul, T. Sema, Preliminary mass transfer performance of CO_2 absorption into AMP-PZ-MEA ternary amines, In: Proceedings of the 15th Greenhouse Gas Control Technologies Conference, 2021, pp. 15-18.
[7] M. Mabuza, K. Premlall, M.O. Daramola, Modelling and thermodynamic properties of pure CO_2 and flue gas sorption data on South African coals using Langmuir Freundlich, Temkin, and extended Langmuir isotherm models, International Journal of Coal Science & Technology 9 (2022) 45.
[8] T. Sema, A. Naami, P. Usubharatana, X. Wang, R. Gao, Z. Liang, R. Idem, P. Tontiwachwuthikul, Mass transfer of CO_2 absorption in hybrid MEA-methanol solvents in packed column, Energy Procedia 37 (2013) 883–889.
[9] B. Xu, H. Gao, X. Luo, H. Liao, Z. Liang, Mass transfer performance of CO_2 absorption into aqueous DEEA in packed columns, Int. J. Greenhouse Gas Control 51 (2016) 11–17.
[10] T. Sema, A. Naami, K. Fu, M. Edali, H. Liu, H. Shi, Z. Liang, R. Idem, P. Tontiwachwuthikul, Comprehensive mass transfer and reaction kinetics studies

of CO_2 absorption into aqueous solutions of blended MDEA–MEA, Chem. Eng. J. 209 (2012) 501–512.
[11] A. Naami, M. Edali, T. Sema, R. Idem, P. Tontiwachwuthikul, Mass transfer performance of CO_2 absorption into aqueous solutions of 4-diethylamino-2-butanol, monoethanolamine, and N-methyldiethanolamine, Ind. Eng. Chem. Res. 51 (2012) 6470–6479.
[12] H. Ling, S. Liu, T. Wang, H. Gao, Z. Liang, Characterization and correlations of CO_2 absorption performance into aqueous amine blended solution of monoethanolamine (MEA) and N, N-dimethylethanolamine (DMEA) in a packed column, Energy Fuel 33 (2019) 7614–7625.
[13] T. Chakravarty, U. Phukan, R. Weilund, Reaction of acid gases with mixtures of amines, Chem. Eng. Prog., (United States) 81 (1985).
[14] D. Barth, C. Tondre, J.-J. Delpuech, Kinetics and mechanisms of the reactions of carbon dioxide with alkanolamines: a discussion concerning the cases of MDEA and DEA, Chem. Eng. Sci. 39 (1984) 1753–1757.
[15] H. Ling, S. Liu, H. Gao, H. Zhang, Z. Liang, Solubility of N_2O, equilibrium solubility, mass transfer study and modeling of CO_2 absorption into aqueous monoethanolamine (MEA)/1-dimethylamino-2-propanol (1DMA2P) solution for post-combustion CO_2 capture, Sep. Purif. Technol. 232 (2020), 115957.
[16] Q. Luo, Q. Zhou, B. Feng, N. Li, S. Liu, A combined experimental and computational study on the shuttle mechanism of piperazine for the enhanced CO_2 absorption in aqueous piperazine Blends, Ind. Eng. Chem. Res. 61 (2022) 1301–1312.
[17] H. Shi, X. Cheng, J. Peng, H. Feng, P. Tontiwachwuthikul, J. Hu, The CO_2 absorption and desorption analysis of tri-solvent MEA+ EAE+ AMP compared with MEA+ BEA+ AMP along with "coordination effects" evaluation, Environ. Sci. Pollut. Res. 29 (2022) 40686–40700.
[18] S. Kumar, M.K. Mondal, Selection of efficient absorbent for CO_2 capture from gases containing low CO2, Korean J. Chem. Eng. 37 (2020) 231–239.
[19] P. Singh, W.P.M. van Swaaij, D.W. Brilman, Kinetics study of carbon dioxide absorption in aqueous solutions of 1, 6-hexamethyldiamine (HMDA) and 1, 6-hexamethyldiamine, N, N′ di-methyl (HMDA, N, N′), Chem. Eng. Sci. 66 (2011) 4521–4532.
[20] P.N. Sutar, P.D. Vaidya, E.Y. Kenig, Activated DEEA solutions for CO_2 capture—A study of equilibrium and kinetic characteristics, Chem. Eng. Sci. 100 (2013) 234–241.
[21] A. Aroonwilas, P. Tontiwachwuthikul, Mass transfer coefficients and correlation for CO_2 absorption into 2-amino-2-methyl-1-propanol (AMP) using structured packing, Ind. Eng. Chem. Res. 37 (1998) 569–575.
[22] H. Quan, S. Dong, D. Zhao, H. Li, J. Geng, H. Liu, CO_2 absorber, Part II: RBFNN and RF model, AIChE Journal 69 (2023), e17904.
[23] M. Afkhamipour, M. Mofarahi, Review on the mass transfer performance of CO_2 absorption by amine-based solvents in low and high-pressure absorption packed columns, RSC Adv. 7 (2017) 17857–17872.
[24] H. Liu, R. Idem, P. Tontiwachwuthikul, Design, Modeling and Simulation of Post Combustion CO_2 Capture Systems Using Reactive Solvents, in: Post-combustion CO_2 Capture Technology, Springer, 2019, pp. 23–27.
[25] S. Dong, H. Quan, D. Zhao, H. Li, J. Geng, H. Liu, Generic AI models for mass transfer coefficient prediction in amine-based CO_2 absorber, Part I: BPNN model, Chemical Engineering Science 264 (2022) 118165.
[26] K. Fu, T. Sema, Z. Liang, H. Liu, Y. Na, H. Shi, R. Idem, P. Tontiwachwuthikul, Investigation of mass-transfer performance for CO_2 absorption into diethylenetriamine (DETA) in a randomly packed column, Ind. Eng. Chem. Res. 51 (2012) 12058–12064.
[27] L. Wen, H. Liu, W. Rongwong, Z. Liang, K. Fu, R. Idem, P. Tontiwachwuthikul, Comparison of overall gas-phase mass transfer coefficient for CO_2 absorption between tertiary amines in a randomly packed column, Chem. Eng. Technol. 38 (2015) 1435–1443.
[28] H. Ling, H. Gao, Z. Liang, Comprehensive solubility of N_2O and mass transfer studies on an effective reactive N, N-dimethylethanolamine (DMEA) solvent for post-combustion CO_2 capture, Chem. Eng. J. 355 (2019) 369–379.
[29] M. Sheng, C. Liu, C. Ge, M. Arowo, Y. Xiang, B. Sun, G. Chu, H. Zou, Mass-transfer performance of CO_2 absorption with aqueous diethylenetriamine-based solutions in a packed column with dixon rings, Ind. Eng. Chem. Res. 55 (2016) 10788–10793.
[30] A.L. Kohl, R. Nielsen, Gas purification, Elsevier, 1997.
[31] G. Astaria, D.W. Savage, A. Bisio, Gas treating with chemical solvents, (1983).
[32] D.W. Green, M.Z. Southard, Perry's chemical engineers' handbook, McGraw-Hill Education, 2019.
[33] D.W. Green, R.H. Perry, Perry's Chemical Engineer Handbook, 8th ed., McGraw-Hill Professional Pub, New York, USA, 2007.
[34] K. Fu, G. Chen, Z. Liang, T. Sema, R. Idem, P. Tontiwachwuthikul, Analysis of mass transfer performance of monoethanolamine-based CO_2 absorption in a packed column using artificial neural networks, Ind. Eng. Chem. Res. 53 (2014) 4413–4423.
[35] H. Liao, H. Gao, B. Xu, Z. Liang, Mass transfer performance studies of aqueous blended DEEA-MEA solution using orthogonal array design in a packed column, Sep. Purif. Technol. 183 (2017) 117–126.
[36] F. Meng, S. Han, Y. Meng, T. Ju, L. Lin, J. Jiang, Effects of hydroxyethyl group on monoethanolamine (MEA) derivatives for biomethane from biogas upgrading, Fuel 325 (2022), 124874.
[37] D. Zhao, S. Dong, L. Bai, D. Li, H. Liu, Experimental method and mathematical method for VLE plots in 3DMA1P-CO_2-H_2O system, Separation and Purification Technology 307 (2023) 122800.
[38] Q. Zeng, Y. Guo, Z. Niu, W. Lin, Mass transfer coefficients for CO_2 absorption into aqueous ammonia solution using a packed column, Ind. Eng. Chem. Res. 50 (2011) 10168–10175.
[39] A. Setameteekul, Statistical factorial design analysis of mass-transfer in carbon dioxide absorption using MEA and MEA/MDEA, Faculty of Graduate Studies and Research, University of Regina, 2006.
[40] K. Onda, H. Takeuchi, Y. Okumoto, Mass transfer coefficients between gas and liquid phases in packed columns, J. Chem. Eng. Jpn. 1 (1968) 56–62.
[41] T. Wang, W. Yu, F. Liu, M. Fang, M. Farooq, Z. Luo, Enhanced CO_2 absorption and desorption by monoethanolamine (MEA)-based nanoparticle suspensions, Ind. Eng. Chem. Res. 55 (2016) 7830–7838.
[42] J.S. Cho, Gas absorption in a countercurrent packed tower:(1) Absorption with simultaneous chemical reaction.(2) Absorption into varying viscous solutions, Oregon State University, 1987.
[43] J. Ying, D.A. Eimer, Measurements and correlations of diffusivities of nitrous oxide and carbon dioxide in monoethanolamine+ water by laminar liquid jet, Ind. Eng. Chem. Res. 51 (2012) 16517–16524.
[44] K. Han, C.K. Ahn, J.Y. Kim, Absorbent characterization for CO_2 capture using wetted-wall column and reaction calorimetry, Energy Procedia 4 (2011) 548–553.
[45] R.E. Dugas, Carbon dioxide absorption, desorption, and diffusion in aqueous piperazine and monoethanolamine, The University of Texas at Austin, 2009.
[46] V. Darde, CO_2 capture using aqueous ammonia, Graduate Schools Yearbook 2010 (2011) 45.
[47] H. Dang, G.T. Rochelle, CO_2 absorption rate and solubility in monoethanolamine/piperazine/water, Sep. Sci. Technol. 38 (2003) 337–357.
[48] J. Ying, D.A. Eimer, Determination and measurements of mass transfer kinetics of CO_2 in concentrated aqueous monoethanolamine solutions by a stirred cell, Ind. Eng. Chem. Res. 52 (2013) 2548–2559.
[49] B.P. Mandal, M. Kundu, S.S. Bandyopadhyay, Physical solubility and diffusivity of N_2O and CO2 into aqueous solutions of (2-amino-2-methyl-1-propanol+ monoethanolamine) and (N-methyldiethanolamine+ monoethanolamine), J. Chem. Eng. Data 50 (2005) 352–358.
[50] S.H. Ali, Kinetics of the reaction of carbon dioxide with blends of amines in aqueous media using the stopped-flow technique, Int. J. Chem. Kinet. 37 (2005) 391–405.
[51] L. Dubois, D. Thomas, CO_2 absorption into aqueous solutions of monoethanolamine, methyldiethanolamine, piperazine and their blends, Chem. Eng. Technol. 32 (2009) 710–718.
[52] A. Dey, A. Aroonwilas, CO_2 absorption into MEA-AMP blend: Mass transfer and absorber height index, Energy Procedia 1 (2009) 211–215.